Co-published by
Institute of Fluid-Flow Machinery
Polish Academy of Sciences
Committee on Thermodynamics and Combustion
Polish Academy of Sciences

http://www.imp.gda.pl/archives-of-thermodynamics/

ARCHIVES OF THERMODYNAMICS

Exergy-Based Performance Assessment of a Solar Air Heater Equipped with Zig-Zag Structured Baffles

Jaya Bohra[a], Vijay Singh Bisht[a], Prabhakar Bhandari[b,c*], Kshitij Pandey[d], Sandeep Singh[e], Ankur Singh Bist[f], Lalit Ranakoti[g], Shivasheesh Kaushik[h], Kapil Kumar Sharma[g]

[a]Department of Thermcal Engineering, Faculty of Technology, Veer Madho Singh Bhandari Uttarakhand Technical University, Dehradun 248007, Uttarakhand, India
[b]Department of Mechanical Engineering, K.R. Mangalam University, Gurugram 122103, Haryana, India
[c]Centre of Excellence-Cyber Security, School of Engineering and Technology, K.R. Mangalam University, Gurugram 122103, Haryana, India
[d]Department of Mechanical Engineering, Uttaranchal University, Dehradun 248007, Uttarakhand, India
[e]O.P. Jindal Global University, Sonipat, 131001, Haryana, India
[f]CSE, Graphic Era Hill University, Bhimtal Campus 263132, Uttarakhand, India
[g]Department of Mechanical Engineering, Graphic Era Deemed to be University, Dehradun 248002, Uttarakhand, India
[h]Department of Mechanical Engineering, Shivalik College of Engineering Dehradun 248197, Uttarakhand, India
*Corresponding author email: prabhakar.bhandari40@gmail.com

Received: 22.12.2025; revised: 19.03.2026; accepted: 30.03.2026

Abstract

By giving the absorber plate artificial roughness, the efficacy of a solar air heater may be increased. A mathematical study has been performed on solar air heaters roughened with Z-shaped baffles. With the help of MATLAB code, an exergy analysis, estimation of exergetic losses and efficiency have been made. The effect of relative pitch ratio for 45° zig-zag structured baffles with a fixed relative blockage height of 0.3 on various exergy parameters has also been studied. The current study has been done for Reynolds numbers ranging from 3000 to 14 000 and for 1100 W/m^2 of solar radiation. It is deduced that with the increase in Reynolds number, the effective efficiency enhances up to a certain point, beyond which it begins to decline. Moreover, the pitch ratio of 1.5 has shown the best performance up to the Reynolds number of 5000, while at higher Reynolds numbers, the pitch ratio of 3 has produced better results.

Keywords: Zig-zag structured baffles; Solar air heater; Absorber plate; Thermal attributes; Exergy investigation

Vol. 47(2026), No. 2, 151–157; doi: 10.24425/ather.2026.158674

Cite this manuscript as: Bohra, J., Bisht, V.S., Bhandari, P. Pandey, K., Singh, S., Bist, A.S., Ranakoti, L., Kaushik, S., & Sharma, K.K. (2026). Exergy-Based Performance Assessment of a Solar Air Heater Equipped with Zig-Zag Structured Baffles. *Archives of Thermodynamics*, 47(2), 151−157.

1. Introduction

Energy plays a significant part in each one's life and is available in numerous forms. As the population around the world and their energy requirements increase, the dependence on conventional fuel also increases. To cope with the demand, the world has started focusing more on renewable or non-conventional resources of energy. Among all types of energy, solar energy has shown the highest potential. A solar air-heater (SAH) is one of the devices that uses sun powered energy. SAH has applications in very vast fields, like in air conditioning, crop drying, etc. [1−3]. As solar air heaters may have low heat transfer rates, researchers try to improve their performance using turbulators. There are several types of turbulators introduced, including inserts/ribs, baffles, fins, delta winglets, vortex generators, etc., that generate turbulence or vortices at walls, resulting in a favourable heat transfer rate with negligible pressure penalty [4,5]. Recent studies on nanoparticle-induced heating demonstrate that

Nomenclature

A – surface area, m²
C – conversion factor
C_d – coefficient of discharge
C_p – specific heat of air, J/(kg·K)
D – hydraulic diameter, m
e – rib height, m
E_{LA} – exergy losses by absorption of irradiation by the absorber, W
E_{Le} – exergy losses by both radiative and convective heat transfer from the absorber, W
$E_{L\Delta P}$ – exergy losses by friction, W
$E_{L\Delta T}$ – exergy losses by the heat transfer to the working fluid, W
f – friction factor for roughened duct
F_o – heat removal factor
h – heat transfer coefficient, W/(m²·K)
H – height of duct, m
I – solar radiation intensity, W/m²
k – thermal conductivity, W/(m·K)
L – length of test section in duct, m
M – mass flow rate of air, kg/s
N – number of glass covers
Nu – Nusselt number
P – pitch, m
P_m – pumping power, W
Pr – Prandtl number
PR – relative roughness pitch
Q_u – useful heat gain, W
Re – Reynolds number
t – thickness, m
T – temperature, K
U_L – head loss coefficients, W/(m²·K)
V – mean flow velocity, m/s
W – width of duct, m

Greek symbols

α – flow angle of attack, °
β – collector inclination to horizontal, °
δ_i – thickness of insulation, m
ΔP – pressure drop, N/m²
ΔT – temperature drop, K
ε – emissivity
η_c – Carnot efficiency
η_{exe} – exergetic efficiency
η_{th} – thermal efficiency of solar collector
λ – wavelength of incident ray, μm
μ – dynamic viscosity of air, N s/m²
ν – kinematic viscosity, m²/s
ρ_a – density of air at mean bulk temperature, kg/m³
σ – Stefan–Boltzmann constant, W/(m²·K⁴)
$(\tau\alpha)$ – transmittance–absorptance product

Subscripts and Superscripts

a – ambient
b – tail
e – collector edge
f – fluid
g – glass cover
i – inlet
m – mean
o – outlet
p – absorber plate
r – roughened
s – smooth
t – head
w – wind

Abbreviations and Acronyms

SAH – solar air heater

optimised materials surface and geometry can significantly enhance heat generation, distribution and convective transport, offering useful design insights for improving thermal performance in solar air heater systems [6,7].

Motivated by the simple yet versatile geometrical characteristics of English alphabet shapes, numerous researchers have investigated the use of alphabet-patterned ribs as artificial roughness elements on the absorber plates of SAH. These rib configurations, modelled after different alphabetic profiles, are designed to disturb the laminar sublayer, enhance turbulence, and promote effective mixing of the air stream near the heated surface [8]. Lau et al. [9] studied V-shaped ribs at various attack angles and observed that 45° and 60° ribs (of relative pitch equal to 10) significantly enhanced heat transfer and flow characteristics compared to smooth and fully-angled ribs, whereas 120° and 135° ribs produced lower heat transfer rates and higher friction losses. They also reported that roughening both opposing walls does not improve overall duct performance. Singh et al. [10,11] studied perforated multi-V-profile ribs in solar air heaters for Reynolds numbers of 2000–18 000, roughness widths of 2–10, and open area ratios up to 0.31. The best performance was obtained at a roughness width of 6 and an open area ratio of 0.27, and they proposed Nusselt and friction factor correlations with accuracies of 12% and 7.5%, respectively.

Lanjewar et al. [12] experimentally showed that W-shaped wire ribs provide better thermo-hydraulic performance than V-shaped ribs in solar air heaters. Ghildyal et al. [13] reported that U-shaped turbulators achieved the highest Nusselt number and overall performance, while D-shaped turbulators produced the greatest friction. In a later study, Ghildyal et al. [14] found that W-contoured turbulators delivered the highest thermal efficiency compared with tapered and reverse-tapered designs (Re = 4000–18 000). Chaudhari et al. [15] reported that inverted L-shaped ribs with a pitch of 17.86 achieved optimal exergy efficiency at 1000 W/m², while Kumar et al. [16] showed performance improvement using a hybrid S-shaped rib-protrusion design. Alhilali et al. [17] observed 2.5–3.0 times higher Nusselt numbers and 2.8–4.4 times greater friction factors with I-shaped ribs in a two-dimensional numerical study of solar air heaters.

Sriromreun et al. [18] experimentally investigated the thermo-hydraulic performance of a rectangular duct with 45° Z-shaped baffles, comparing in-phase and out-of-phase arrangements, as shown in Fig. 1. The in-phase configuration produced stronger turbulence and higher heat transfer rates, but also increased friction losses. Based on the results, empirical correlations for the Nusselt number and friction factor were developed for similar roughened duct designs. Bohra et al. [19] investigated the influence of geometric parameters, i.e. blockage ratio on the thermal performance of SAH equipped with Z-shaped baffles mounted on the absorber plate. They reported the best thermal performance achieved at a blockage ratio of 0.3.

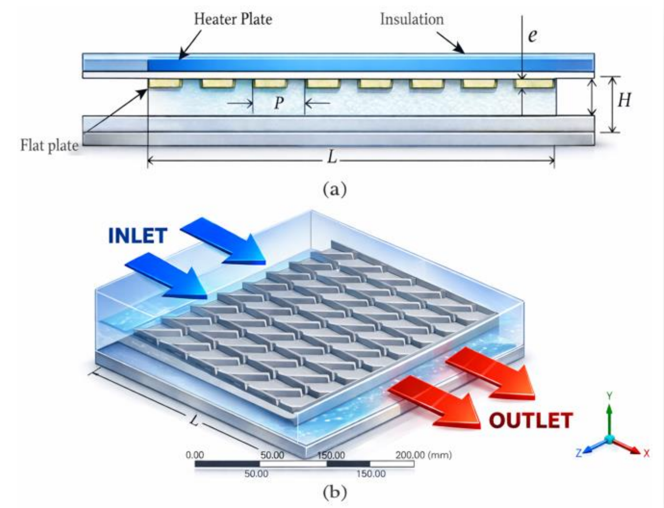

Fig. 1. (a) Cross sectional view of solar air heater; (b) zig-zag structured baffle arrangement.

The present research work introduces a pioneering investigation into the synergistic impact of exergy analysis and the implementation of zig-zag structured baffles in solar air heater systems. Unlike conventional studies that primarily rely on energy analysis, this research employs exergy analysis, providing a more comprehensive evaluation of energy utilisation and losses. The integration of zig-zag structured baffles represents a novel design modification aimed at optimising heat transfer within the solar air heater. The innovative zig-zag configuration promotes turbulent flow, thereby enhancing the interaction between the air and absorber plate. By combining these two innovative elements, the research aims to achieve a breakthrough in solar air heater efficiency, offering a holistic and advanced approach to the design and optimisation of sustainable solar heating technologies.

The primary objective of the research is to systematically investigate and quantify the impact of incorporating zig-zag structured baffles having different relative roughness pitch on the performance of solar air heater systems using exergy analysis. Through this research, the goal is to provide a comprehensive understanding of the flow of energy, losses and efficiencies within the solar air heater, surpassing traditional energy analyses. The specific focus on exergy analysis aims to identify and address inefficiencies and opportunities for improvement that may not be apparent in conventional energy assessments. Additionally, by introducing the novel element of zig-zag structured baffles, the research seeks to assess and optimise heat transfer mechanisms within the solar air heater, ultimately contributing valuable insights towards enhancing the overall efficiency and effectiveness of solar air heating technologies.

2. Materials and methods

In the current attempt, exergetic evaluation has been investigated for the solar heater having zig-zag structured baffles in the plate. Table 1 gathers the information on SAH characteristics and the operating constraints.

Table 1. Boundary conditions, variables and operational conditions employed in analytical computations.

Parameters	Range of values
Rectangular channel total length (*L*)	700 mm
Channel width (*W*)	300 mm
Channel height (*H*)	25 mm
Transmittance-absorptance $(\tau\alpha)$	0.8
Emittance of glass (e_g)	0.88
Emittance of plate (e_p)	0.9
Glass cover thickness (t_g)	4 mm
Number of glass covers (*N*)	1
Thickness of insulation (t_i)	50 mm
Thermal conductivity of insulation (K_i)	0.037 W/(m K)
Wind velocity (V_w)	1 m/s
Relative roughness pitch (*PR*)	1.5-3
Uniform heat flux or insolation (*I*)	1000 W/m²
Inlet temperature of air (T_a)	300K

MATLAB program has been used to evaluate different exergetic parameters. The correlations for the Nusselt number (Nu) and friction factor (*f*) for the duct of rectangular shape having zig-zag structured baffles are shown in Eqs. (1) and (2), respectively [18]

$$\mathrm{Nu} = 0.29023\mathrm{Re}^{0.669891}\mathrm{Pr}^{0.4}\left(\frac{e}{H}+1\right)^{4.854282}\mathrm{Pr}^{0.4}\left(\frac{P}{H}+1\right)^{-0.47904}, \quad (1)$$

$$f = 0.237223\mathrm{Re}^{-0.0726}\left(\frac{e}{H}+1\right)^{9.859262}\left(\frac{P}{H}+1\right)^{-0.86932}. \quad (2)$$

The total or overall loss coefficient is expressed as:

$$U_L = U_t + U_b + U_e, \quad (3)$$

where U_t, U_b and U_e are the head loss coefficient, tail loss coefficient and side loss coefficient, respectively.

The useful gain in energy is expressed as:

$$Q_{u1} = [I(\tau\alpha) - U_L(T_{ap} - T_s)]A_p. \quad (4)$$

where T_{ap} and T_s are the temperatures of the absorber plate and the surroundings.

Equation (5) expresses another method for estimating a usable energy gain:

$$Q_{u2} = F_o[I(\tau\alpha) - U_L(T_o - T_i)]A_p, \quad (5)$$

where F_o denotes the heat removal factor, T_o and T_i are the temperatures of the outflow and inlet air, respectively.

Ideally, the values Q_{u1} and Q_{u2} would be equal. Nonetheless, only when the variance between the two values is more than 0.1% of Q_{u1}, the absorber plate temperature has been altered. In the MATLAB code, a conditional loop has been employed till the condition is satisfied. A uniform heat flux of 1000 W/m² is commonly applied in SAH numerical studies to represent a realistic and controlled solar irradiation condition on the absorber plate. This value corresponds to typical peak solar insolation under clear-sky conditions, making it a practical reference for performance analysis. Using a constant heat flux also simplifies the boundary conditions, allowing direct comparison between different rib configurations by ensuring that any change in thermal performance is solely due to geometric modifications rather than variations in heat input [15,20]. The tabular presentation in Table 2 outlines the thermo-physical characteristics of the absorber plate material, namely, aluminium, and the surrounding air.

Table 2. Boundary condition and thermo-physical properties of absorber plate material and air.

Properties	Air	Aluminium
Density	1.176 kg/m³	2719 kg/m³
Specific heat	1006.4 J/(kg K)	871 J/(kg K)
Thermal conductivity	0.02624 W/(m K)	202.4 W/(m K)
Viscosity	1.857e-05 kg/(m s)	---

Thereafter, key performance parameters such as exergetic losses and overall exergy efficiency were evaluated for different pitch ratios. The analysis considered four major sources of exergy destruction: (i) losses associated with solar irradiation absorption at the absorber plate, (ii) losses due to combined radiative and convective heat transfer from the absorber plate to the ambient environment, (iii) losses occurring during heat transfer from the absorber plate to the working fluid, and (iv) losses arising from fluid friction within the duct. This comprehensive evaluation enabled a clearer understanding of how pitch ratio influences the thermodynamic performance of the solar air heater.

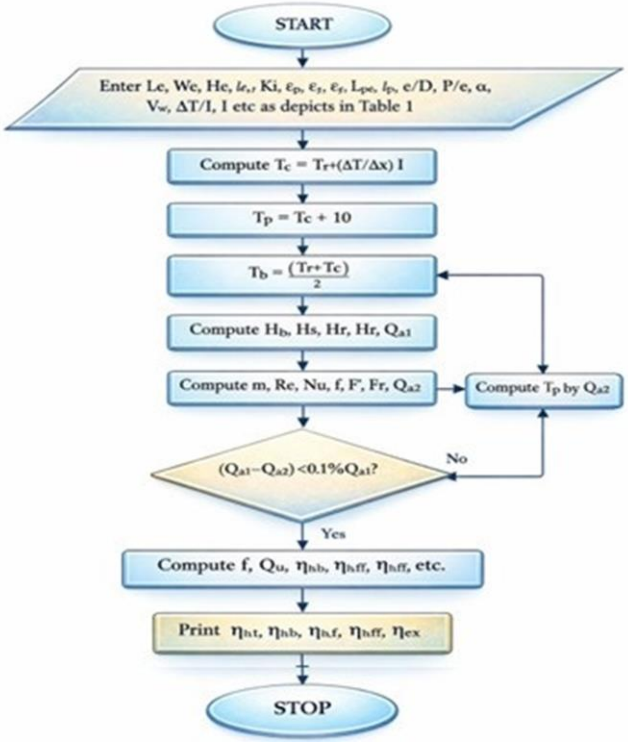

Fig. 2. Flowchart of the assumed mathematical model.

The flowchart in Fig. 2 depicts the step-by-step process followed in the current numerical work.

The expressions given in Eqs. (6)–(11) follow the approach presented by Bohra et al. [19]. Exergy losses by friction are determined by:

$$E_{L\Delta P} = \frac{m}{\rho} \Delta P \frac{T_a}{T_{fm}}. \tag{6}$$

Exergy losses by heat transfer to the working fluid are calculated by:

$$E_{L\Delta T} = A_p \, \eta_{th} \left(\frac{T_a}{T_{fm}} - \frac{T_a}{T_{pm}} \right). \tag{7}$$

Exergy losses by both radiative and convective heat transfer from the absorber to the atmosphere are calculated by:

$$E_{Le} = U_L A_p (T_{pm} - T_a) \left(1 - \frac{T_a}{T_{pm}} \right). \tag{8}$$

Exergy losses by absorption of irradiation by the absorber are calculated as:

$$E_{LA} = I \, A_p \, (\tau\alpha) \, \eta_{exe} - \left(1 - \frac{T_a}{T_{pm}} \right). \tag{9}$$

The exergetic efficiency is calculated as:

$$\eta_{exe} = \frac{E_n}{E_s}, \tag{10}$$

where E_n and E_s are the net exergy flow and exergy input, respectively. The effective efficiency (η_{eff}) is calculated as: .

$$\eta_{eff} = \frac{Q_u - P_m/C}{I \, A_p}. \tag{11}$$

3. Results and discussion

The addition of zig-zag structured baffles to a solar air heater can improve its thermal performance. However, this augmentation is always accompanied by increased friction losses. Due to that, the net energy gain will reduce, and it is always desirable to select the optimum design parameters. The influence of pitch ratio for Reynolds numbers ranging from 3000 to 14 000 has been studied. All configurations of pitch ratio were studied for a constant blockage height ratio of 0.3, insolation of 1100 W/m^2 and attack angle of 45°.

3.1. Exergy losses

Exergy losses due to friction are determined by the factor that produces increased friction losses. The lower the temperature rise parameter, the higher the mass flow rate, and thus the larger the friction losses. Figure 3 depicts the fluctuation of exergetic losses via friction with the temperature.

It was discovered that the most exergetic losses occur at lower pitch ratios. The value of exergetic losses via friction ($E_{L\Delta P}$) then increases as the temperature rise parameter decreases. It was observed that exergy losses due to friction are minimised after the temperature ascent criterion ($\Delta T/I$) of 0.004.

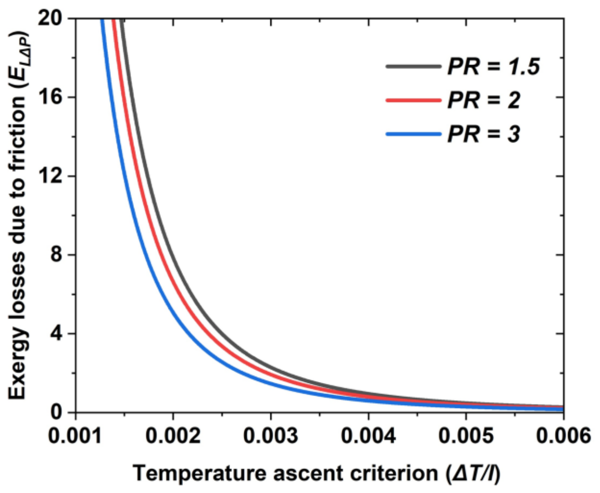

Fig. 3. Variation of exergy losses due to friction ($E_{L\Delta P}$) with temperature ascent criterion ($\Delta T/I$).

Exergy losses by absorption (E_{LA}) are due to irradiation absorbed by the plate of absorber at the mean temperature (T_{pm}), and as the temperature ($\Delta T/I$) increases, E_{LA} is found to decrease, as shown in Fig. 4. It was observed that the pitch ratio of 3 has shown the least value of E_{LA}. The irreversibility rises as the temperature rise parameter increases, resulting in higher exergy losses. The absorber plate's temperature rises in lockstep with the temperature rise parameter. For all pitch ratios, E_{LA} rises with the temperature ascent criterion, but eventually begins to decline.

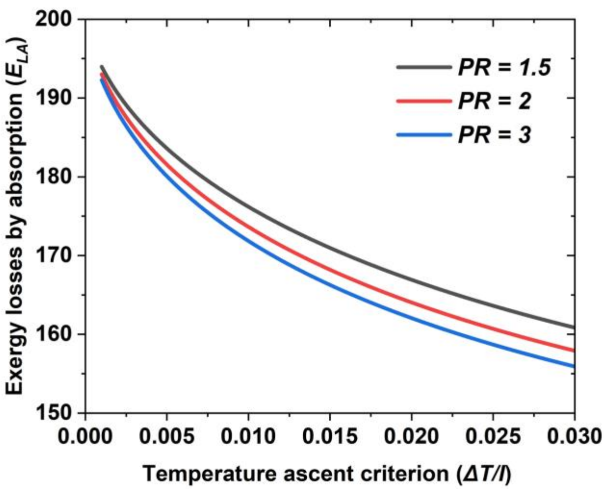

Fig. 4. Variation of exergy losses (E_{LA}) with temperature ascent criterion.

As the temperature rise parameter is increased, there is a corresponding increase in irreversibility, leading to higher exergy losses. The absorber plate temperature also elevates with the escalation of the temperature rise parameter. Consequently, the maximum exergetic losses occur when the temperature rise parameter has a higher value. The variation of exergy loss due to the working fluid with the temperature ascent criterion ($\Delta T/I$) shows a similar trend for all pitch ratios (PR) in Fig. 5. At low values of $\Delta T/I$, the exergy loss increases sharply, indicating enhanced useful energy transfer to the fluid as the temperature difference grows. The curves reach a peak around $\Delta T/I \approx 0.01$–0.015, where the exergy transfer is maximised. Beyond this point, a gradual decline is observed for all PR values, suggesting that a higher temperature ascent leads to increased irreversibilities and reduced effective exergy transfer. Among the cases, PR = 1.5 exhibits the highest peak exergy loss, followed by PR = 3 and PR = 2, while at larger $\Delta T/I$ values, PR = 2 maintains comparatively higher exergy loss than the others. Overall, the results indicate the existence of an optimum temperature ascent criterion for maximising exergy transfer to the working fluid, which slightly varies with the pitch ratio.

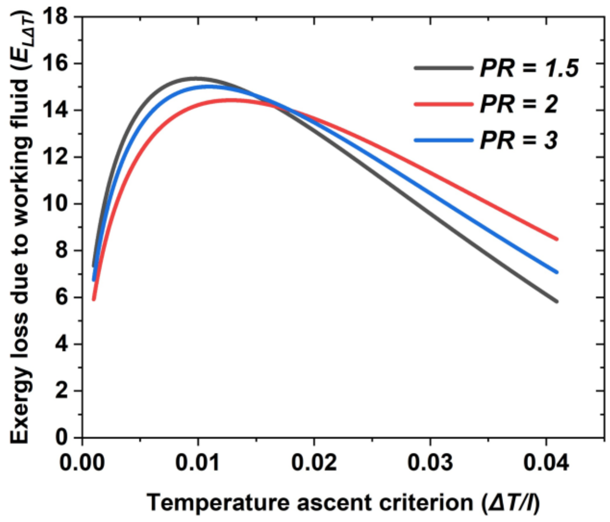

Fig. 5. Variation of exergy losses by working fluid ($E_{L\Delta T}$) with temperature ascent criterion.

Figure 6 shows the variation of exergy deficit to the surroundings (E_{Le}) with the temperature rise parameter. It has been acknowledged that with an increment in temperature rise parameter, exergy loss to the environment also rises because of the greater temperature differential between the absorber plate and the environment. Moreover, the pitch ratio of 3 has shown a maximum E_{Le} followed by the pitch ratios 2 and 1.5.

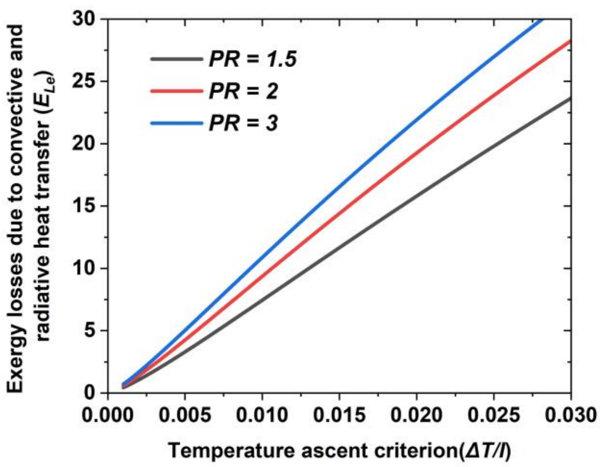

Fig. 6. Variation of exergy losses with temperature ascent criterion by convective and radiative heat transfer (E_{Le}).

3.2. Exergetic efficiency

Figure 7 shows how the exergetic efficiency (η_{exe}) varies with the temperature ascent criterion ($\Delta T/I$) for diverse pitch ratios. Due to the extremely high mass flow rate, a lower $\Delta T/I$ value concludes in a negative adverse value of exergetic efficiency. The exergetic efficiency improves as the value of $\Delta T/I$ increases. The pitch ratio 3 has the lowest exergetic efficiency, while the pitch ratio 1.5 has the highest exergetic efficiency. This is due to the supremacy of mechanical power, or the power necessary to overcome frictional forces.

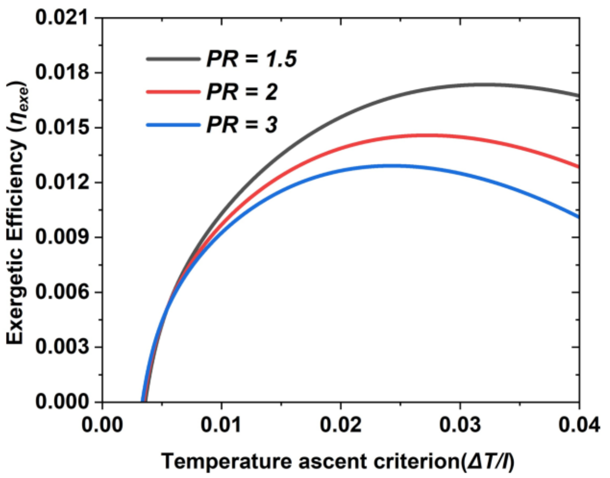

Fig. 7. Variation of exergetic efficiency (η_{exe}) with the temperature ascent criterion.

3.3. Effective efficiency

Figure 8 illustrates the variation of effective efficiency (η_{eff}) with Reynolds number for different pitch ratio (*PR*) configurations at a constant relative blockage ratio of 0.3, insolation of 1100 W/m², and attack angle of 45°.

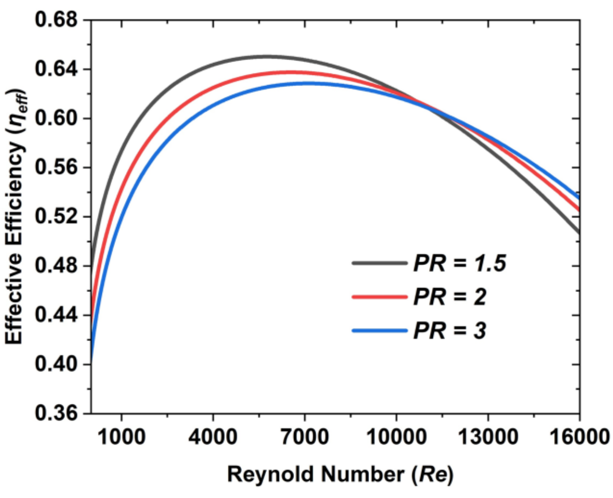

Fig. 8. Variation of η_{eff} with Re for various pitch proportions.

It is observed that the effective efficiency increases with the Reynolds number, reaches a peak, and then gradually declines at higher flow rates. The initial rise in efficiency is due to improved convective heat transfer at higher Reynolds numbers, whereas the subsequent decline is caused by the increasing mechanical power required to overcome frictional losses.

At lower Reynolds numbers, the configuration with *PR* = 1.5 demonstrates the highest effective efficiency, attaining a maximum of about 64% at Re ≈ 5000. This trend continues up to approximately Re = 11 000, where *PR* = 1.5 maintains superior performance compared to other configurations. However, beyond this point, the efficiency for *PR* = 1.5 decreases more rapidly, and the configuration with *PR* = 3 exhibits comparatively better performance at higher Reynolds numbers. This indicates that lower pitch ratios are more effective at moderate flow conditions, while higher pitch ratios become advantageous at elevated Reynolds numbers due to reduced frictional penalties.

4. Conclusions

The numerical investigation demonstrates that the incorporation of zig-zag structured baffles significantly influences the exergetic and effective performance of the solar air heater over the Reynolds number range of 3000–14 000.

Exergy analysis reveals that frictional losses are the highest at lower pitch ratios, while exergy transfer to the working fluid reaches a maximum at a temperature ascent criterion of about $\Delta T/I \approx 0.01–0.015$.

Among the tested configurations, *PR* = 1.5 shows the highest exergetic efficiency, whereas *PR* = 3 results in the lowest efficiency due to reduced turbulence intensity.

In terms of effective efficiency, *PR* = 1.5 achieves the maximum value of approximately 64% at Re ≈ 5000 and maintains superior performance up to about Re ≈ 11 000. Beyond this range, the efficiency of *PR* = 1.5 declines more rapidly, and *PR* = 3 performs better at higher Reynolds numbers due to comparatively lower frictional penalties.

Overall, the results indicate that a lower pitch ratio is optimal for moderate flow conditions, while a higher pitch ratio becomes advantageous at elevated Reynolds numbers.

References

1. Kumar, A., Karn, A., McGregor, C., & Singh, V.P. (2025). A critical analysis of paradigm shifts from domestic solar cooking to institutional solar cooking technologies. *Renewable and Sustainable Energy Reviews*, 218, 115840. doi: 10.1016/j.rser.2025.115840
2. Al-Yasiri, Q., Szabó, M., & Arıcı, M. (2022). A review on solar-powered cooling and air-conditioning systems for building applications. *Energy Reports*, 8, 2888–2907. doi: 10.1016/j.egyr.2022.01.172
3. Bisht, V.S., Patil, A.K., & Gupta, A. (2018). Review and performance evaluation of roughened solar air heaters. *Renewable and Sustainable Energy Reviews*, 81, 954–977. doi: 10.1016/j.rser.2017.08.036
4. Saini, R.P., & Singal, S.K. (2007). A review on roughness geometry used in solar air heaters. *Solar Energy*, 81, 1340–1350. doi: 10.1016/j.solener.2007.01.017
5. Chamoli, S., Thakur, N.S., & Saini, J.S. (2012). A review of turbulence promoters used in solar thermal systems. *Renewable and Sustainable Energy Reviews*, 16, 3154–3175. doi: 10.1016/j.rser.2012.01.021

6. Radomski, P., Ziółkowski, P., de Sio, L., & Mikielewicz, D. (2021). Computational fluid dynamics simulation of heat transfer from densely packed gold nanoparticles to isotropic media. *Archives of Thermodynamics*, 42(3), 87–113. doi: 10.24425/ather.2021.138111
7. Ziółkowski, P., Radomski, P., Koulali, A., Kreft, D., Barański, J., & Mikielewicz, D. (2025). Numerical study of heat transfer intensification in a chamber with heat generating by irradiated gold nanorods: One-way multiphysics and multiscale approach. *Energies*, 19(1), 181. doi: 10.3390/en19010181
8. Bisht, V.S., Singh, D.B., Kumar, P., Jain, S., Bhandari, P., Mumtaz, M.A., & Rahman, M.H. (2026). Innovative spherical turbulator configurations for enhanced solar air heater performance: A numerical and analytical study. *Energy*, 342, 139601. doi: 10.1016/j.energy.2025.139601
9. Lau, S., Kukreja, R., & McMillin, R. (1991). Effects of V-shaped rib arrays on turbulent heat transfer and friction of fully developed flow in a square channel. *International Journal of Heat and Mass Transfer*, 34(7), 1605–1616. doi: 10.1016/0017-9310(91)90140-A
10. Singh, V., Jain, S., & Gupta, J. (2023). Analysis of the effect of perforation in multi-V rib artificial roughened single-pass solar air heater: Part A. *Experimental Heat Transfer*, 36(2), 163–182. doi: 10.1080/08916152.2021.1988761
11. Singh, V., Jain, S., & Kumar, A. (2023). Establishment of correlations for thermo-hydraulic parameters due to perforation in a multi-V rib roughened single-pass solar air heater. *Experimental Heat Transfer*, 36(5), 597–616. doi: 10.1080/ 08916152.2022.2064940
12. Lanjewar, A., Bhagoria, J.L., & Sarviya, R.M. (2011). Heat transfer and friction in solar air heater duct with W-shaped rib roughness on absorber plate. *Energy*, 36, 4531–4541. doi: 10.1016/j.energy.2011.03.054
13. Ghildyal, A., Bisht, V.S., Rawat, K.S., & Bhandari, P. (2023). Effect of D-shaped, reverse D-shaped and U-shaped turbulators in solar air heater on thermo-hydraulic performance. *Archives of Thermodynamics*, 44(2), 3–20. doi: 10.24425/ather.2023.146556
14. Ghildyal, A., Bisht, V.S., Bhandari, P., Thapliyal, S., Kaushik, S., Ranakoti, L., Bangari, R.S., Srivastav, A., Kanojia, N., & Paul, A.R. (2024). A comparative numerical evaluation of solar air heater performance having W-contoured, taper-contoured and reverse taper-contoured turbulators. *Archives of Thermodynamics*, 45(4), 189–196. doi: 10.24425/ather.2024.152008
15. Chaudhari, M., Sharma, S.L., & Debbarma, A. (2023). Exergetic performance analysis of solar air heater with inverted L-shape ribs as roughness element. *Archives of Thermodynamics*, 44(3), 241–267. doi: 10.24425/ather.2023.147546
16. Kumar, S., Bisht, V.S., Bhandari, P., Ranakoti, L., Negi, A., Bist, A.S., & Padalia, D. (2025). Computational analysis of modified solar air heater having combination of ribs and protrusion in S-shaped configuration. *International Journal on Interactive Design and Manufacturing*, 19(5), 3467–3478. doi: 10.1007/s12008-024-01972-2
17. Alhilali, H.A.A., Al-Chlaihawi, K., Zarzoor, A.K., & Flayyih, M.A. (2025). Optimization of thermohydraulic parameters in solar air heater ducts featuring I-shaped ribs. *Heat Transfer*, 54, 3790–3814. doi: 10.1002/htj.23384
18. Sriromreun, P., Thianpong, C., & Promvonge, P. (2012). Experimental and numerical study on heat transfer enhancement in a channel with Z-shaped baffles. *International Communications in Heat and Mass Transfer*, 39(7), 945–952. doi: 10.1016/j.icheatmasstransfer.2012.05.016
19. Bohra, J., Bisht, V.S., Bhandari, P., Rawat, K.S., Singh, J., Kumar, K., & Rawat, B. (2022). Effect of variable blockage height ratio on performance for solar air heater roughened with 45°-shaped baffles. *Materials Today: Proceedings*, 69(2), 153–157. doi: 10.1016/j.matpr.2022.08.279
20. Singh, J., Bisht, V.S., Bhandari, P., Kumar, K., Singh, J., Alam, T., Dixit, S., Singh, S., & Khusnutdinov, R. (2023). Computational parametric investigation of solar air heater with dimple roughness in S-shaped pattern. *International Journal on Interactive Design and Manufacturing*, 18(5), 2969–2979. doi: 10.1007/s12008-023-01392-8